


# Calibrating CGH Substrate TWE and Simulating Adjustment Error in Cylindrical Surface Measurement

Linghua Zhang, Sen Han , Xianyu Wu, Xianhao Qi, Jun Cheng, and Chunfeng Xu

**Abstract**—Computer-generated hologram (CGH) is a diffractive optical element that has been commonly used as wavefront corrector in the interferometer and can be accurately manufactured to meet the requirements of high-precision detection. But the transmitted wavefront error (TWE) of the CGH substrate and the adjustment errors of cylindrical surface are influence factors of high accuracy measurement. In this paper, we propose the method of calibrating the CGH substrate TWE. After calibrating, the substrate TWE is  $0.0052\lambda$  (RMS). Meanwhile, we obtain the general expression for the misalignment aberrations by describing the relationship between the wavefront of the measured cylindrical mirror and the corresponding adjustment errors. Then the adjustment errors of the test cylindrical surface can be completely separated by subtracting the fitting function from the measurement on the basis of least-square algorithm. After that, the PV value changes from  $3.0565\lambda$  to  $0.9825\lambda$ , and the RMS value changes from  $0.5278\lambda$  to  $0.1273\lambda$ , the measurement results have been greatly improved.

**Index Terms**—Adjustment errors, CGH, cylindrical mirror, transmitted wavefront error.

## I. INTRODUCTION

CYLINDER is a special aspheric surface, and is widely used because of its unique optical imaging characteristics, such as using cylindrical lenses to correcting some ophthalmic diseases in ophthalmology, laser beam shaping in laser science [1], wide-screen projectors in film equipment, and high-energy laser expansion [2], beam alignment, and imaging scanning [3], etc. All these applications demand much higher accuracy of shape of the cylindrical surface. Generally, in order to gain high accuracy in cylindrical testing, a piece of high-quality CGH (computer generated hologram) is inserted behind transmission flat to generate specified wave-front to match measured cylinder. Whereas, owing to the inserting the CGH, the CGH errors and the alignment of measured cylinder become the main problems in the interferometric measurement.

On the one hand, the CGH errors can be design errors, alignment errors, or fabrication errors. The design of CGH can be

Manuscript received March 2, 2022; revised April 1, 2022; accepted April 6, 2022. Date of publication April 12, 2022; date of current version April 28, 2022. This work was supported by the National Natural Science Foundation of China under Project 62127901. (Corresponding author: Sen Han.)

The authors are with the University of Shanghai for Science and Technology, Yangpu District 200093, China (e-mail: 15250121530@163.com; 1206690210@qq.com; wuxianyu202@163.com; 13035085171@163.com; chengjun\_usst@163.com; xucf@usst.edu.cn).

Digital Object Identifier 10.1109/JPHOT.2022.3166557

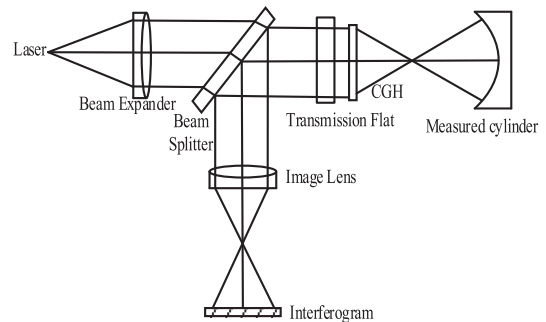


Fig. 1. The Fizeau interferometer with CGH compensator.

achieved by Zemax or other program, so that the design error is not difficult problem [4]. With the aid of alignment hologram, the location of CGH can be well aligned. CGH can be manufactured by e-beam writing or laser direct writing with high-precision and high-resolution [5], but there are some unknown factors during the fabrication process. In this paper, we focus on the CGH substrate TWE, which is dominant in the cylindrical wavefront. Ping Zhou *et al.* extended the parametric model, classified CGH fabrication errors, and proposed the measurement methods for fabrication errors in the CGH substrate, duty cycle, etching depth and effect of surface roughness, respectively [6]. However, the effects of all these fabrication errors are coupled together, and it is difficult to decouple the individual effects of each error source on the wavefront [7]. So, we propose a method to calibrate the CGH substrate TWE.

On the other hand, the errors introduced by adjustment of measured cylindrical mirror also affect the cylindrical measurement accuracy. Small misalignment errors are unavoidable due to the mechanical tolerance of the adjustment stage. Therefore, it is necessary to eliminate these additional aberrations according to the measurement data. We employ a mathematical expression to describe the misadjustment errors introduced by the rotation and shift during the measurement process, and present a least-square algorithm to subtract the misalignment aberrations from the measurement results.

## II. PRINCIPLE

As shown in Fig. 1, the CGH transforms an incoming plane wave into a perfect cylindrical wave and incidents perpendicularly onto the measured cylinder. Then the reflected wave

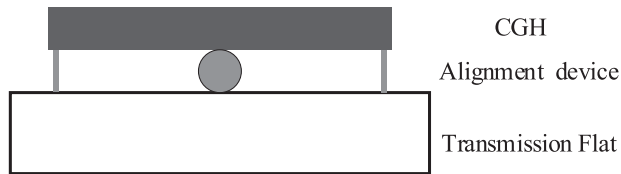


Fig. 2. The dedicated equipment of CGH and transmission flat.

second passes through the CGH, which carries the information of deviations from measured cylinder, and returns into the interferometer. Obviously, the entire measurement system requires an exact alignment between the interferometer, the CGH and the measured cylinder [3], [8]. If we use six-dimensional adjustment frame to adjust the relative position between CGH and interferometer, it will be complex and introduce some alignment errors simultaneously [9], [10]. Thus, we employ alignment hologram of the CGH to align CGH. At the same time, we provide a dedicated equipment for controlling the translation and the rotation of the CGH, as shown in the Fig. 2, connecting the CGH to the transmission flat for avoiding misalignment errors, which not only can adjust the tilt and rotation of the CGH, but also can realize the alignment between CGH and the transmission flat.

### III. DISCUSSIONS

#### A. The Calibration of the CGH Substrate TWE

When used to perform null test, the CGH is in the measurement optical path, as shown in Fig. 1, CGH errors will compromise the accuracy of the interferometric measurements. The CGH errors have design errors, alignment errors, or fabrication errors. The CGH fabrication errors can be classified into five types: substrate errors, pattern distortion errors, duty-cycle errors, etching depth errors and surface roughness errors [4]. Among all the fabrication errors, the substrate error is dominant and is typically of low spatial frequency. Substrate error usual means substrate surface variation from its ideal shape and can be measured by using a testing beam or a collimated beam [5]. Usually method is to subtract the non-zero order surface measurement from the zero order measurement, and the CGH substrate error can be correctly removed [9], [11]. However, the method has its limitation, because the wavefront error of the CGH apart from the CGH substrate error, other fabrication errors also affect the zero-order measurement. These errors affect zero and nonzero orders differently. Although the wavefront errors caused by the substrate error can be totally removed using this method, there are residual errors from the CGH substrate wavefront. Hence, we calibrate the CGH substrate TWE based on the method.

In order to avoid the influence of spherical aberration, we choose high-precision flat mirror to generate parallel beam for wavefront calibration. The calibration setups are illustrated in Fig. 3. A Fizeau interferometer, a transmission flat (TF), and two return flats (RF1, RF2) are used to calibrate the CGH substrate TWE. Four measurements are made: the RF1 with CGH in the Fizeau cavity is first tested, the RF1 without CGH is second measured, the RF2 with CGH is third tested, and

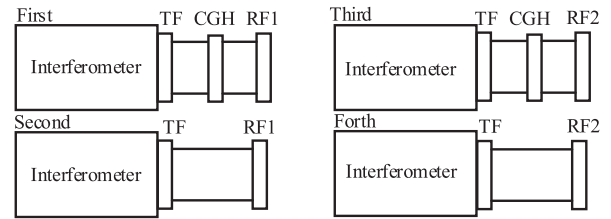


Fig. 3. The calibration of CGH substrate TWE.

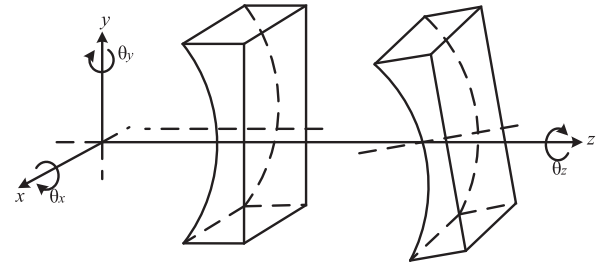


Fig. 4. The schematic diagram of the cylinder misalignment state.

the RF2 without CGH is forth detected. The difference of the first and second measurement mainly depicts the CGH substrate error, which can be written as T1. The difference of the first and second measurement, which can be written as T1, mainly depicts the CGH substrate error. But in fact, the substrate error is so coupled with other fabrication errors that it is difficult to measurement separately. So we add third measurement and forth measurement, instead of the first and the second test, RF1 is replaced with RF2 that is also a high precision return flat. Subtracting T1 from third measurement should theoretically be the same as forth measurement, whereas there is a deviation in actual measurements. The deviation comes from residual wavefront errors of CGH substrate.

#### B. Adjustment Errors of Measured Cylinder

After completing the alignment of the CGH and transmission flat, even though we use six-dimensional adjustment frame to adjustment the cylinder, there are still adjustment errors due to the mechanical tolerance of the adjustment frame [10]. Compared with the detection of plane and sphere, cylinder has six degrees of freedom, namely [12]:  $x$ -axis translation,  $y$ -axis translation,  $z$ -axis translation, rotation around the  $x$ -axis (tilt), rotation around the  $y$ -axis (tilt), and rotation around the  $z$ -axis, as shown in the Fig. 4, and requires more rotation and translation in the adjustment process, which is bound to increase difficulty of cylindrical measurement. Therefore, it is necessary to analyze the adjustment aberrations caused by rotation and shifting in the cylindrical interference detection, and eliminate these additional aberrations according to the measurement data.

For normal-incidence interferometric testing of cylindrical surface, the translations along the cylinder axis create no aberrations. So, we will analyze the adjustment errors in five degrees of freedom.

To simplify the analysis, assuming the cylindrical equation at the ideal location is described by (1) [13], where  $r$  is the radius of curvature of the tested cylindrical wavefront, the origin of

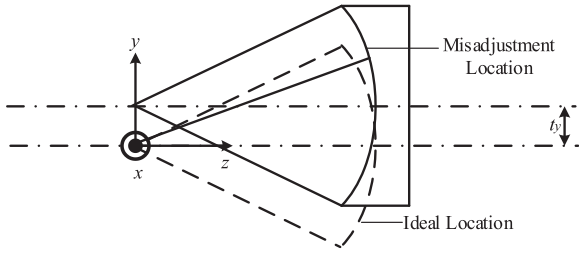


Fig. 5. The cylinder translates along the positive direction of the y-axis.

the coordinate system o-xyz is located at the focal axis of the cylindrical wave:

$$y^2 + z^2 = r^2 \quad (1)$$

Supposing that the adjustment errors of the cylindrical measurement results are independent of each other, then the misadjustment errors caused by the measured cylinder can be expressed as:

$$W_{mis} = \Delta W_{t_y} + \Delta W_{t_z} + \Delta W_{\theta_x} + \Delta W_{\theta_y} + \Delta W_{\theta_z} \quad (2)$$

1) *Adjustment Error Introduced by the Translation Along the Y-Axis:* Fig. 5 shows the small translation of relative to ideal location

The cylindrical wavefront of ideal location can be written as:

$$\begin{aligned} W_r &= \sqrt{r^2 - y^2} \\ &= r \sqrt{1 - \frac{y^2}{r^2}} \approx r - \frac{1}{2} \cdot \frac{y^2}{r} - \frac{1}{8} \cdot \frac{y^4}{r^3} - \frac{1}{16} \cdot \frac{y^6}{r^5} \end{aligned} \quad (3)$$

when there is a translation of  $t_y$  along the y-axis, the misadjustment cylindrical wavefront is:

$$\begin{aligned} W_{t_y} &= \sqrt{r^2 - (y - t_y)^2} \\ &\approx r + \left(\frac{t_y}{r}\right) y - \left(\frac{1}{2r}\right) y^2 + \left(\frac{t_y}{2r^3}\right) y^3 \\ &\quad - \left(\frac{1}{8r^3}\right) y^4 + \left(\frac{3t_y}{8r^5}\right) y^5 - \left(\frac{1}{16r^5}\right) y^6 \end{aligned} \quad (4)$$

The adjustment error introduced after the measured cylinder is translated along the y-axis can be given by:

$$\Delta W_{t_y} = -2t_y \left( \frac{y}{r} + \frac{y^3}{2r^3} + \frac{3y^5}{8r^5} \right) \quad (5)$$

2) *Adjustment Error Introduced by the Translation Along the Z-Axis:* Fig. 6 shows the case in which there is a displacement of relative to the ideal location, it is easy to see that the radius of curvature of the ideal cylindrical wavefront and misadjustment cylindrical wavefront is different.

So, the misadjustment cylindrical wavefront is given by:

$$W_{t_z} = t_z + \sqrt{r^2 - y^2} = t_z + r - \frac{y^2}{2r} - \frac{y^4}{8r^3} - \frac{y^6}{16r^5} \quad (6)$$

And the cylindrical wave of ideal location is:

$$W_r = t_z + r + t_z - \frac{y^2}{2(r + t_z)} - \frac{y^4}{8(r + t_z)^3} - \frac{y^6}{16(r + t_z)^5} \quad (7)$$

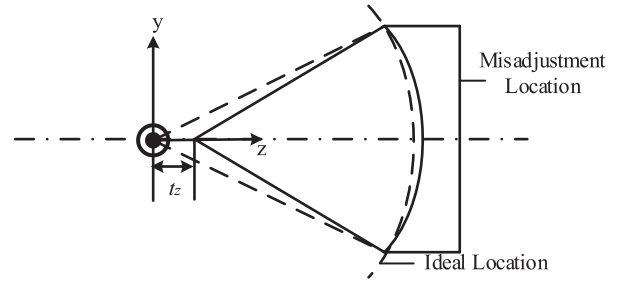


Fig. 6. The cylinder moves along the positive direction of the z-axis.

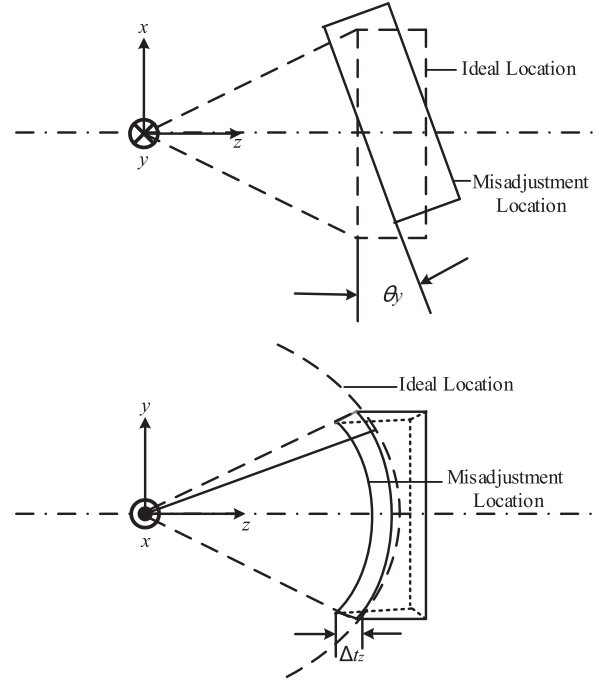


Fig. 7. a) The top view of the cylinder rotating around the y-axis, b) The three-dimensional view of the cylinder rotating around the y-axis.

Error introduced after translating  $t_z$  along the z-axis can be written as:

$$\Delta W_{t_z} = t_z \left( 2 + \frac{y^2}{r^2} + \frac{3y^4}{4r^4} + \frac{5y^6}{8r^6} \right) \quad (8)$$

3) *Adjustment Error Introduced by the Rotation Along the Y-Axis:* Fig. 7 shows a small amount of rotation  $\theta_y$  along the y-axis, it can be observed that the  $\theta_y$  rotation does not introduce a translation in the y-axis, but introduces  $\Delta t_z$  translation along the z-axis, and

$$\Delta t_z = x \cdot \tan \theta_y \quad (9)$$

Cylindrical wavefront after rotating around the y-axis:

$$\begin{aligned} W_{\theta_y} &= \Delta t_z + r + \Delta t_z - \frac{y^2}{2(r + \Delta t_z)} \\ &\quad - \frac{y^4}{8(r + \Delta t_z)^3} - \frac{y^6}{16(r + \Delta t_z)^5} \end{aligned} \quad (10)$$

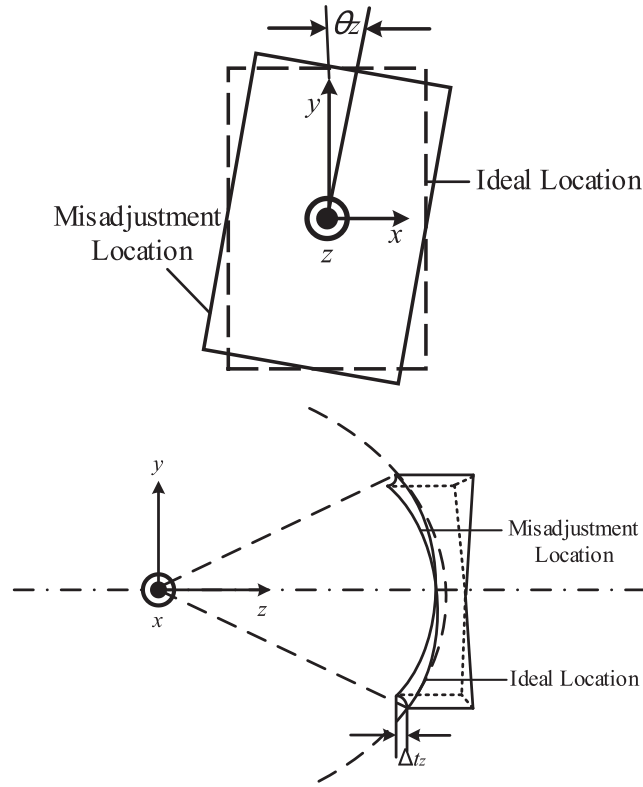


Fig. 8. a) The side view of the cylinder rotating around the z-axis, b) The three-dimensional view the cylinder rotating around the z-axis.

The adjustment error introduced is expressed as:

$$\Delta W_{\theta_y} = \tan \theta_y \left( 2x + \frac{xy^2}{r^2} + \frac{3xy^4}{4r^4} + \frac{5xy^6}{8r^6} \right) \quad (11)$$

4) *Adjustment Error Introduced by Rotation Around the Z-Axis:* The cylinder to be measured rotates  $\theta_z$  around the z-axis relative to the ideal location. It can be seen from the Fig. 8 that the rotation  $\theta_z$  does not produce displacement along the z-axis, but introduces translation  $\Delta t_y$  in the y-axis, and  $\Delta t_y = x \cdot \tan \theta_z$ .

Cylindrical wavefront after rotating around the z-axis is represented as:

$$W_{\theta_z} = r + \left( \frac{x \cdot \tan \theta_z}{r} \right) y - \left( \frac{1}{2r} \right) y^2 + \left( \frac{x \cdot \tan \theta_z}{2r^3} \right) y^3 - \left( \frac{1}{8r^3} \right) y^4 + \left( \frac{3x \cdot \tan \theta_z}{8r^5} \right) y^5 - \left( \frac{1}{16r^5} \right) y^6 \quad (12)$$

Adjustment error introduced by rotation around the z-axis can be expressed as:

$$\Delta W_{\theta_z} = -2x \tan \theta_z \left( \frac{y}{r} + \frac{y^3}{2r^3} + \frac{y^5}{8r^5} \right) \quad (13)$$

5) *Adjustment Error Introduced by Rotation Around the X-Axis:* The cylinder to be measured rotates  $\theta_x$  around the x-axis relative to the ideal location. As can be seen from the Fig. 9, the amount of rotation  $\theta_x$  introduces a displacement  $\Delta t_y$  along the y-axis,  $\Delta t_y = r \cdot \sin \theta_x \cos \theta_x$ , and a displacement  $\Delta t_z$  along the z-axis,  $\Delta t_z = r \cdot \sin \theta_x \sin \theta_x$ .

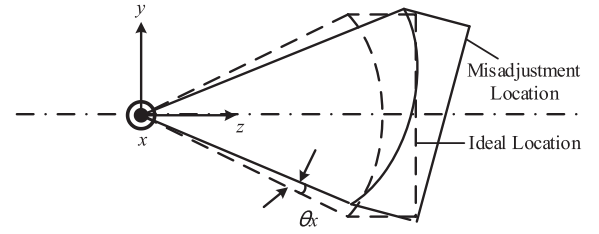


Fig. 9. Cylinder rotates around the x-axis.

When  $\theta_x$  is very small,  $\sin \theta_x \approx \theta_x$ ,  $\cos \theta_x \approx 1$ , Cylindrical wavefront after rotating around the x-axis is given by:

$$W_{\theta_x} = r \cdot \theta_x^2 + r + y \cdot \theta_x - \left( \frac{1}{2r} \right) y^2 + \left( \frac{\theta_x}{2r^2} \right) y^3 - \left( \frac{1}{8r^3} \right) y^4 + \left( \frac{3\theta_x}{8r^4} \right) y^5 - \left( \frac{1}{16r^5} \right) y^6 \quad (14)$$

Adjustment error introduced by rotation around the x-axis can be represented as:

$$\Delta W_{\theta_x} = r \cdot \theta_x^2 + y \cdot \theta_x + \left( \frac{\theta_x}{2r^2} \right) y^3 + \left( \frac{3\theta_x}{8r^4} \right) y^5 \quad (15)$$

Finally the misalignment errors  $W_{mis}$  can be expressed as a linear combination of adjustment errors of five degrees of freedom:

$$\begin{aligned} W_{mis} &= \Delta W_{t_y} + \Delta W_{t_z} + \Delta W_{\theta_x} + \Delta W_{\theta_y} + \Delta W_{\theta_z} \\ &= -2t_y \left( \frac{y}{r} + \frac{y^3}{2r^3} + \frac{3y^5}{8r^5} \right) + t_z \left( 2 + \frac{y^2}{r^2} + \frac{3y^4}{4r^4} + \frac{5y^6}{8r^6} \right) \\ &\quad + r \cdot \theta_x^2 + y \cdot \theta_x + \left( \frac{\theta_x}{2r^2} \right) y^3 + \left( \frac{3\theta_x}{8r^4} \right) y^5 \\ &\quad + x \cdot \tan \theta_y \left( 2 + \frac{y^2}{r^2} + \frac{3y^4}{4r^4} + \frac{5y^6}{8r^6} \right) \\ &\quad - 2x \cdot \tan \theta_z \left( \frac{y}{r} + \frac{y^3}{2r^3} + \frac{3y^5}{8r^5} \right) \end{aligned} \quad (16)$$

The five parameters  $t_y$ ,  $t_z$ ,  $\theta_x$ ,  $\theta_y$ , and  $\theta_z$  can be estimated based on the least-squares fitting algorithm, which means the variance  $V$  has a minimum value, i.e., to make the partial derivatives of  $t_y$ ,  $t_z$ ,  $\theta_x$ ,  $\theta_y$ , and  $\theta_z$  must be zeros [3], [12], [14], [15].

$$V = \sum (W - W_{mis})^2 \quad (17)$$

where  $W$  represents the actual measurement result. By subtracting  $W_{mis}$  from  $W$ , then the corrected phase values  $\varphi$  is obtained, here  $\varphi$  can be regard as the actual surface deviation.

$$\varphi = W - W_{mis} \quad (18)$$

In order to determine the sensitivity of adjustment errors, the five adjustment degrees of freedom are respectively applied to a certain increments of adjustment, where the translation along the y-axis starts from 0.001 mm and increases to 0.005 mm; the translation along the z-axis starts from 0.01 mm and increases to 0.05 mm; the rotation around the x-axis starts from 0.01°

TABLE I  
INTERFEROGRAMS OF ADJUSTMENT ERRORS CAUSED BY THE OF FIVE  
DEGREES OF FREEDOM

	0.001mm	0.002mm	0.003mm	0.004mm	0.005mm
$t_y$					
	0.01mm	0.02mm	0.03mm	0.04mm	0.05mm
$t_z$					
	0.01°	0.02°	0.03°	0.04°	0.05°
$\theta_x$					
	0.001°	0.002°	0.003°	0.004°	0.005°
$\theta_y$					
$\theta_z$					

and increase to  $0.05^\circ$ ; the rotation around the y-axis starts from  $0.001^\circ$  and increase to  $0.005^\circ$ ; the rotation around the z-axis starts from  $0.001^\circ$  and increases to  $0.005^\circ$ . The interferograms acquired under the different adjustment state are exhibited in Table I.

It can be obtained from Table I that slight adjustments in different directions of the measured cylinder will make a difference in the test wavefront. In other words, the sensitivity of the cylindrical measurement is different at different degrees of freedom. Especially in the adjustment caused by the translation, the translation along the y-axis is more sensitive than that along the z-axis. In the adjustment introduced by the rotation, the adjustment around x-axis is also less sensitive than the rotation around y-axis and z-axis. Therefore, during the test process, attention must be paid to the translation along the y-axis and the rotation around the z-axis. In addition, it can be noticed that the same type of interference fringes is formed by the rotation around the x-axis and the translation along the z-axis, which have the same distribution of optical path differences. This means that two adjustment errors are coupled to each other, and the adjustment between the two have the same effect.

#### IV. EXPERIMENTAL RESULTS

A Fizeau interferometer with a 6 inch aperture transmission flat (TF) has been used in the experiment, the test system is shown in Fig. 10, in which a CGH cylinder null with a 140 mm aperture and F/5.5 is positioned in front of the interferometer, which can transform an incident plane wave into the reference cylindrical wavefront. A cylindrical mirror with 285 mm curvature radius was tested in this experiment. Since the device has



Fig. 10. The test system of cylinder.

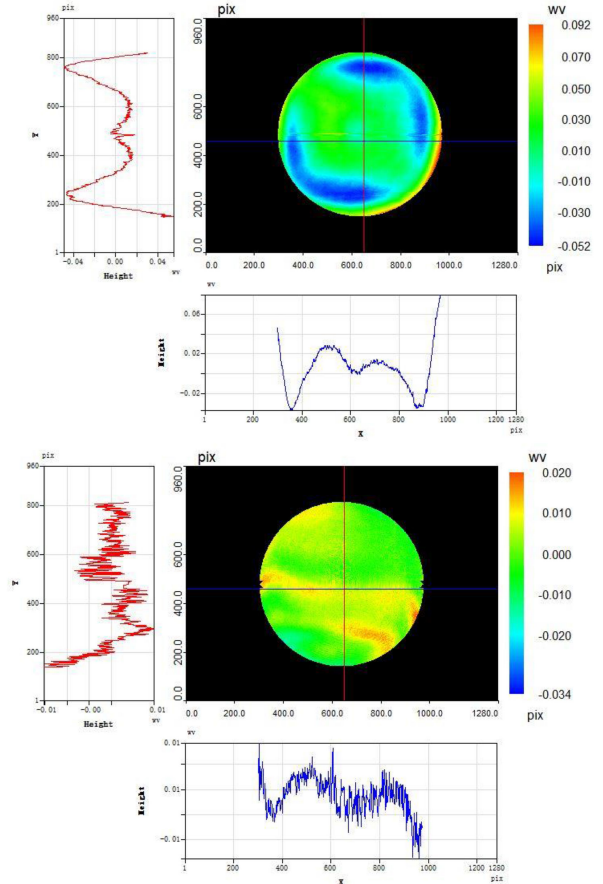


Fig. 11. The result of CGH substrate error and the calibrated TWE, a) the result of CGH substrate error, b) the result of calibrated TWE.

been used to align the CGH with the interferometer, only the alignment of the measured cylinder is required.

According to description presented in Section III-A, the four measurements are achieved, shown in the Table II.

The difference between the first measurement and the second measurement represents mainly the CGH substrate error, as demonstrated in Fig. 11(a). We find that the difference between the third measurement and the substrate error is different from the fourth measurement, and this deviation is the CGH substrate TWE,  $0.0052\lambda$  (RMS), as shown in Fig. 11(b).

Meanwhile, the interferogram and the measured phase map of the measured cylindrical mirror are shown in Fig. 12(a) and Fig. 12(b), which shows the cylindrical measurement results after eliminating the CGH substrate error, with the peak-to-valley (PV) value is  $3.0565\lambda$  and the root mean square (RMS) value is  $0.5278\lambda$ .

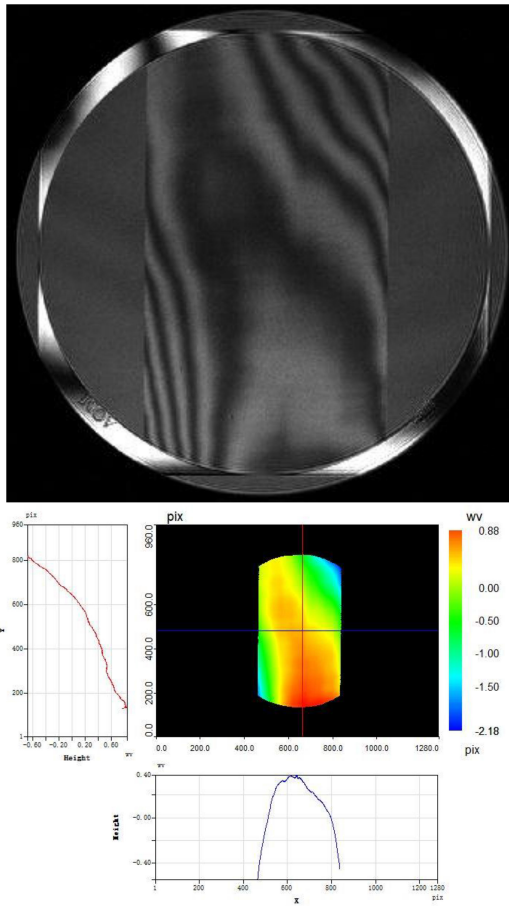


Fig. 12. The measurement results after removing the CGH substrate error, a) the interferogram of measured cylinder, b) the phase map of the measured cylinder.

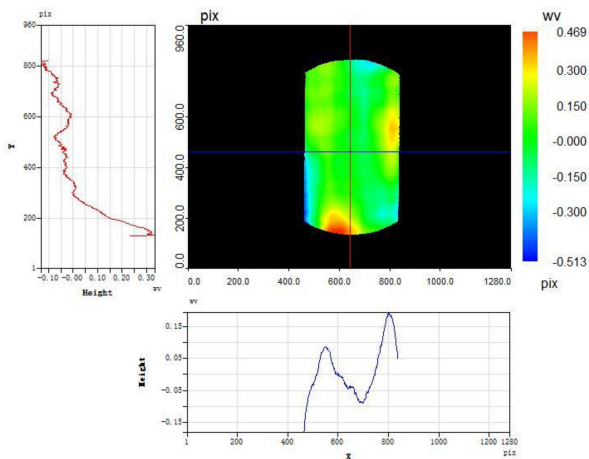


Fig. 13. The result after eliminating the adjustment errors.

After that, the adjustment errors of the measured cylinder can be subtracted from the measured wavefront, then the relevant deviations of the test cylindrical part from the ideal figure are obtained. Fig. 13 are the result of the cylinder measurement after eliminating the adjustment error. The PV and RMS values for this measurement result are  $0.9825\lambda$  and  $0.1273\lambda$ , respectively. After the misadjustment error is eliminated through the algorithm, the PV value changes from  $3.0565\lambda$  to  $0.9825\lambda$ , and

TABLE II  
THE FOUR STEPS MEASUREMENTS OF CALIBRATION

	RMS( $\lambda$ )	PV( $\lambda$ )
First	0.0291	0.1597
Second	0.0086	0.0444
Third	0.0249	0.1959
Forth	0.0046	0.0357
Third-substrate error	0.0059	0.0951

TABLE III  
THE REPEATABILITY OF CYLINDRICAL MEASUREMENT

	RMS( $\lambda$ )	PV( $\lambda$ )
1	0.127	0.982
2	0.127	0.978
3	0.127	1.023
4	0.128	0.998
5	0.127	1.009
6	0.111	0.966
7	0.112	1.057
8	0.112	1.053
9	0.112	1.009
10	0.112	1.057
STD	0.008	0.034

the RMS value changes from  $0.5278\lambda$  to  $0.1273\lambda$ . It can be seen that the measurement results after eliminating the adjustment errors of cylinder are significantly improved.

In order to verify the stability and repeatability of the system, repeating the measurement on the cylinder several times. Table III shows the PV value and RMS value of each measurement, as well as their standard deviations. By calculating the standard deviation of the ten sets of measurements, the repeatability of the cylinder test is obtained, as shown in the Table III, the repeatability of PV value is 0.034 and the repeatability of RMS value is 0.008.

## V. CONCLUSION

We remove the substrate error of CGH by subtracting the first-order wavefront from the zero-order one and on this basis, and continue to calibrate the CGH substrate TWE. After calibration, the substrate TWE is  $0.0052\lambda$  (RMS). Meanwhile, we derive the mathematical descriptions for the possible adjustment errors and separate the adjustment errors of cylindrical surface based on the least-square algorithm. We observed that the cylinder measurements have been improved by TWE calibration and misadjustment errors removal.

## REFERENCES

- [1] W. Wei and P. J. Guo, "Optical testing of cylindrical surfaces with computer-generated holograms," in *Proc. Int. Symp. Photoelectronic Detection Imag.*, 2013, Art. no. 89120T.
- [2] Y. Zhao and Y. Gong, "New design of beam expanding unit for excimer laser," *Opt. Lasers Eng.*, vol. 50, no. 9, pp. 1202–1208, 2012.
- [3] J. Peng *et al.*, "Calibration of misalignment aberrations in cylindrical surface interferometric measurement," in *Proc. SPIE Opt. Meas. Syst. Ind. Inspection VIII*, 2013, Art. no. 878829.

- [4] H. Lin, S. Chen, and X. Shuai, "Characterization of the contribution of CGH fabrication error to measurement uncertainty in null test," in *Proc. AOPC, Optoelectron. Micro/Nano-Opt.*, 2017, Art. no. 104601O.
- [5] A. G. Poleshchuk, V. P. Korolkov, R. K. Nasyrov, and J. M. Asfour, "Computer generated holograms: Fabrication and application for precision optical testing," in *Proc. Opt. Fabr., Testing, Metrol. III*, 2008, Art. no. 710206.
- [6] Z. Ping and B. J. H., "Fabrication error analysis and experimental demonstration for computer-generated holograms," *Appl. Opt.*, vol. 46, no. 5, pp. 657–663, 2007.
- [7] F. Jie, D. Chao, and T. Xing, "Error analysis for aspheric surface testing system," in *Proc. ISPDI - 5th Int. Symp. Photoelectronic Detection Imag.*, 2013, Art. no. 7656.
- [8] S. Scheiding *et al.*, "Freeform mirror fabrication and metrology using a high performance test CGH and advanced alignment features," in *Proc. SPIE - Int. Soc. Opt. Eng.*, 2013, Art. no. 8613.
- [9] Z. Chunyu and B. J. H., "Optical testing with computer generated holograms: Comprehensive error analysis," in *Proc. SPIE, Opt. Manuf. Testing X*, 2013, Art. no. 8838.
- [10] Q. Wang, Y. Yu, and K. Mou, "Method for the fabrication error calibration of the CGH used in the cylindrical interferometry system," in *Proc. Soc. Photo-Opt. Instrum. Engineers Conf. Ser.*, 2016, Art. no. 101551Z.
- [11] P. Zhou, "Error analysis and data reduction for interferometric surface measurements," *Dissertations Thesis Gradworks*, 2009.
- [12] P. Junzheng, Ge Dongbao, Yu Yingjie, W. Kesheng, and C. Mingyi, "Method of misalignment aberrations removal in null test of cylindrical surface," *Appl. Opt.*, vol. 52, no. 30, pp. 7311–7323, 2013.
- [13] H. Yaa, *Research On Absolute Detection Technology of Conjugate Difference Surface Shape Based on Zero Interference*. Jiangsu, China: Nanjing Univ. Sci. Technol., 2018.
- [14] Q. Chen *et al.*, "Separating misalignment from mis figure in stigmatic null tests of conic mirrors," in *Proc. SPIE - Int. Soc. for Opt. Eng.*, 2010, Art. no. 7849.
- [15] L. Wei *et al.*, "Separation of misalignment aberrations in interferometric testing for the surface measurement of the frustum of a cone," *Appl. Opt.*, vol. 58, no. 36, pp. 9734–9739, 2019.